La granJa:
Revista de
Ciencias de la Vida
pISSN:1390-3799; eISSN:1390-8596
https://doi.org/10.17163/lgr.n41.2025.01

Special Issue / Edición Especial

Conectivity Corridors

Analysis and prediction of land use/land cover change in the Llanganates-Sangay Connectivity Corridor by 2030

Análisis y predicción del cambio de uso y cobertura de suelo en el Corredor de Conectividad Llanganates-Sangay para 2030

Luis Jaramillo[1,2], Andrea Mancheno Herrera[1,6], Adriana Guzmán*[3,4,6] and Juan Gabriel Mollocana Lara*[5]

[1] *World Wildlife Fund (WWF) Ecuador, Código Postal 170517, Quito, Ecuador.*
[2] *Nippon Koei Latin America- Caribbean Co. Ltd., Código Postal 170526, Quito, Ecuador.*
[3] *Facultad de Recursos Naturales. Escuela Superior Politécnica de Chimborazo ESPOCH, Código Postal EC060155, Riobamba, Ecuador.*
[4] *Centro de Estudios Integrales de Dinàmica Exògena CEIDE. Universidad Nacional de La Plata, Código Postal 1900, La Plata, Argentina.*
[5] *Grupo de Investigación Ambiental en el Desarrollo Sustentable GIADES, Ingeniería Ambiental. Universidad Politécnica Salesiana UPS, Quito, 170702, Ecuador.*
[6] *Red de Investigación del Corredor Ecológico Llanganates Sangay.*

*Corresponding author: catalina.guzman@espoch.edu.ec, jmollocana@ups.edu.ec

Received on October 1st, 2024. Accepted, after revision on February 14th, 2025. Published on March 1st, 2025.

Abstract

This paper analyses Land Use and Land Cover (LULC) change trends in the Llanganates-Sangay Connectivity Corridor (CELS) from 2018 to 2022 and predicts trends through 2030. MapBiomas LULC maps reveals annual change rates (2018–2022) of -0.37%/year (-1147.33 ha) for Forest Formation, -1.17%/year (-30.01 ha) for Non-Forest Natural Formation, 2.21%/year (906.19 ha) for Agriculture and Livestock Areas, 8.50%/year (250.84 ha) for Non-Vegetated Areas, and 0.17%/year (30.31 ha) for Water Bodies. The higher annual change rate inside Forest Formation is -0.58%/year (-990.35 ha) occurring in areas not designated under any conservation status. Projections for 2030 were made using the MOLUSCE tool, combining an Artificial Neural Network (ANN) model with Cellular Automata simulations. The ANN model was trained on five explanatory variables and LULC maps from 2018 and 2020, achieving a training error of 8.46%. Predictive accuracy was assessed by comparing the simulated 2022 LULC map with the 2022 MapBiomas map, resulting in a Kappa coefficient of 0.95, indicating excellent predictive accuracy. Additionally, LULC simulations from 2022 to 2030 predict annual rates of change of –0.27%/year (-1628.97 ha) for Forest Formation, -1.39%/year (-63.49 ha) for Non-Forest Natural Formation, 1.92%/year (1778.26 ha) for Agriculture and Livestock Areas, 0.97%/year (30.38 ha) for Non-Vegetated Areas, and 0.63%/year (-146.18 ha) for Water Bodies. The findings show that annual rates of deforestation will remain low and protected areas will have less deforestation than non-protected areas.

Keywords: Deforestation, CELS, MOLUSCE, LULC changes.

Resumen

Este estudio analiza las tendencias de cambio de uso y cobertura del suelo (LULC) en el Corredor de Conectividad Llanganates-Sangay (CELS) durante el período 2018-2022 y predice tendencias hasta 2030. Los mapas de LULC de MapBiomas revelan tasas anuales de cambio (2018-2022) de -0,37 %/año (-1147.33 ha) para Formación de Bosque, -1,17 %/año (-30,01 ha) para Formaciones Naturales No Boscosas, 2,21 %/año (906.19 ha) para Áreas de Agricultura y Ganadería, 8,50 %/año (250,84 ha) para Áreas sin Vegetación y 0,17 %/año (30,31 ha) para Cuerpos de Agua. La mayor tasa de cambio anual dentro de Formación de Bosque, -0,58 %/año (-990,35 ha), ocurre en áreas no protegidas. Las proyecciones para 2030 se realizaron utilizando la herramienta MOLUSCE, que combina una Red Neuronal Artificial (ANN) con simulaciones de Autómatas Celulares. La ANN fue entrenada con cinco variables explicatorias y mapas de LULC de 2018 y 2020, logrando un error de entrenamiento de 8,46 %. La precisión predictiva se evaluó comparando el mapa simulado de LULC para 2022 con el mapa de MapBiomas 2022, obteniendo un coeficiente Kappa de 0,95, lo que indica una excelente precisión. Además, las simulaciones de LULC para 2022-2030 predicen tasas anuales de cambio de -0,27 %/año (-1628,97 ha) para Formación de Bosque, -1,39 %/año (-63,49 ha) para Formaciones Naturales No Boscosas, 1,92 %/año (1778,26 ha) para Áreas de Agricultura y Ganadería, 0,97 %/año (30,38 ha) para Áreas No Vegetadas y 0,63 %/año (-146,18 ha) para Cuerpos de Agua. Los resultados sugieren que las tasas anuales de deforestación se mantendrán bajas y que las áreas protegidas tendrán menos deforestación que las áreas que no están protegidas.

Palabras clave: Deforestación, CELS, MOLUSCE, cambios de cobertura y uso de suelo.

Suggested citation: Jaramillo, L., Mancheno Herrera, A., Guzmán, A. and Mollocana Lara, J.G. (2025). Analysis and prediction of land use/land cover change in the Llanganates-Sangay Connectivity Corridor by 2030. *La Granja: Revista de Ciencias de la Vida.* Vol. 41(1):11-31. https://doi.org/10.17163/lgr.n41.2025.01.

Orcid IDs:

Luis Jonathan Jaramillo Coronel: https://orcid.org/0000-0002-3127-9855
Andrea Cecilia Mancheno Herrera: https://orcid.org/0009-0000-5525-1665
Adriana Catalina Guzmán Guaraca: https://orcid.org/0000-0003-0473-2041
Juan Gabriel Mollocana Lara: https://orcid.org/0000-0002-2430-8400

1 Introduction

Ecuador is known worldwide as one of the 13 most biodiverse countries in the world, but it faces a growing threat, as between 1990 and 2000 the country lost 15% of its native forest area, leading to one of the highest deforestation rates in Latin America (Rivas et al., 2024). This dynamic mainly affects the Amazon, considered one of the most biodiverse regions on the planet (Mainville et al., 2006). Forest losses compromise the country's capacity to keep global warming below 1.5°C, since this region stores between 367 and 733 Gt of CO_2 in its vegetation and soils (Vergara et al., 2022).

Deforestation and land use change have caused an accelerated fragmentation of natural vegetation areas in the Andes and the Ecuadorian Amazon. Between 1990 and 2018, with the main affected areas being the buffer zones of protected areas, 25.5% were lost in their surroundings (Kleemann et al., 2022). These dynamics compromise the effectiveness of conservation strategies, even in areas with high levels of protection. Fragmentation affects the provision of essential ecosystem services, such as water regulation, carbon storage and biodiversity conservation.

In this context, it is crucial to implement comprehensive measures that include forest conservation and sustainable management of buffer zones (Vergara et al., 2022). Nowadays, tools based on remote sensing and artificial intelligence allow progress in the analysis and prediction of LULC changes, both spatially and temporally. Classification techniques such as Random Forest (RF) and Support Vector Machines (SVM) have demonstrated high accuracy in the generation of land use and land cover mapping, facilitating the observation and analysis of deforestation processes and LULC transformation (Admas, 2024; Elagouz et al., 2020; Lukas et al., 2023; Tikuye et al., 2023).

In this study, we also used the *QGIS add-on MOLUSCE* (Modules for Land Use Change Evaluation), which combines spatial and temporal data with advanced modeling techniques, such as cellular automata (CA) and artificial neural networks (ANN). This tool allows simulating and predicting changes in land use and land cover. MOLUSCE has demonstrated its effectiveness in various contexts (Muhammad et al., 2022; Talukdar et al., 2020). The Llanganates-Sangay Connectivity Corridor (CELS) is a critical ecological link, connecting Llanganates National Park in the north, Sangay National Park in the south and several conservation areas recognized under diverse schemes within its boundaries. The CELS encompasses a significant ecotone, bridging the Andean highlands and the Amazon basin, and playing a pivotal role in preserving the region's unique ecosystems (Ríos-Alvear et al., 2024).

Relevant scientific research has been developed for more than 150 years in this area, with important results, such as the identification of 178 species of orchids and nearly 200 species of endemic plants, surpassing even the Galapagos Islands in botanical diversity (Jost, 2004). It is also home to nearly 700 species of birds and 285 species of reptiles and amphibians, surpassing the records of Yasuní National Park (INABIO et al., 2023). However, human activities have reshaped this area. For instance, late colonization processes in cities like Baños and Puyo, driving human settlement and economic activities such as tourism and agriculture, have significantly influenced land use changes in the region, leading to the conversion of natural areas into agricultural and urban spaces (Herrera and Rodríguez, 2016). Deforestation and LULC change have increased landscape fragmentation and significantly reduced ecosystem connectivity, putting the survival of species and the provision of ecosystem services at risk (Reyes-Puig et al., 2023).

This study aims to determine land use and land cover changes in the Llanganates-Sangay Connectivity Corridor (CELS) from 2018 to 2022 and project trends up to 2030 using the MOLUSCE tool. It focuses on quantifying forest cover loss during the analysis period and forecasting future scenarios of change in LULC, based on changes recorded between 2018 and 2022.

2 Materials and Methods

2.1 Study area

The Llanganates-Sangay Connectivity Corridor (CELS) spans the provinces of Tungurahua, Pastaza, and Morona Santiago (Figure 1) and encompasses 92,148 hectares (Viteri-Basso et al., 2024). The corridor serves as an ecological link, connecting Llanganates National Park in the north with Sangay National Park in the south. It forms a key transition zone between the eastern Andes and the western Amazon. This area was designated as a "Gift to the Earth" by WWF in 2002, recognizing its global importance for biodiversity. The CELS was officially recognized as a Connectivity Corridor in 2023 by Ecuador's Ministry of Environment and Natural Resources (Ríos-Alvear et al., 2024).

The CELS ranges in altitude from 760 and 3812 meters above sea level and has a rainy tropical climate (Viteri-Basso et al., 2024), with annual precipitation between 2500 and 5500 mm and temperatures ranging between 9 and 22°C. These climatic and altitudinal variations favor the formation of habitats that foster exceptional biodiversity (Gaglio et al., 2017; Ríos-Alvear et al., 2024). This area plays an important role in providing water resources for the Pastaza and Napo River basins that are vital for local communities, agricultural and tourism activities, and hydroelectric energy generation (Gaglio et al., 2017).

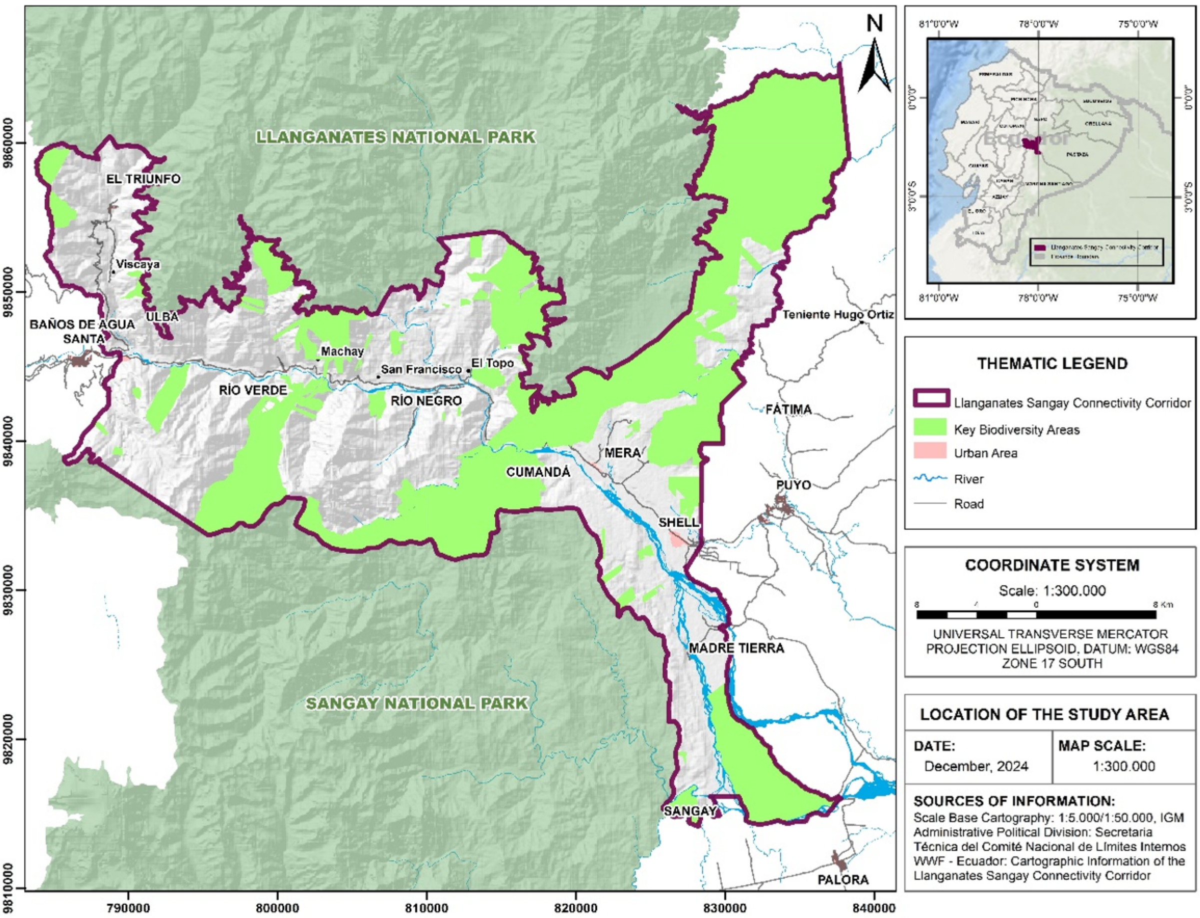

Figure 1. Location map of the CELS.

The primary economic activities in this area include agriculture, cattle ranching, tourism, fish farming, and timber production. While these activities are critical to the local economy, they have significantly impacted ecosystems, leading to deforestation and habitat fragmentation (Delgado Fernández et al., 2023).

Over the past two decades, various conservation initiatives have been implemented in this area, led by local, national, and international organizations such as EcoMinga Foundation, local governments, the Ministry of Environment, Water and Ecological Transition of Ecuador (MAATE), WWF, among others. Ecotourism initiatives within CELS can be found in the geoportal *https://geocels-upsq.hub.arcgis.com/*

Conservation strategies have included, for instance, the establishment of officially recognized protected areas, the management of privately conserved areas not officially recognized but designated for ecosystem conservation, and collaboration with local communities to promote sustainable land management practices. The latter includes supporting the adoption of agroecological practices to prevent soil degradation, maintain fertility, and curb agricultural frontier expansion (Aneloa et al., 2024). Additionally, nature-based tourism has been boosted as a sustainable development strategy to enhance local livelihoods while preserving natural ecosystems.

Despite these efforts, there remains the need to further integrate local communities into sustainable management strategies that effectively balance socioeconomic development with environmental conservation (Alvarado, 2020; Aneloa et al., 2024).

2.2 Data collection

Satellite imagery is essential for monitoring rainfall, deforestation, land use changes, and environmental impacts (Perea-Ardila et al., 2021). However, the high cloud cover in the Ecuadorian Amazon, located within the intertropical convergence zone, limits spatial data availability (Heredia-R et al., 2021). To address this, *MapBiomas* Collection 1.0 (MapBiomas, 2024) was chosen for its extensive temporal coverage (1985–2022) and ability to avoid a cloud cover category, which occupies nearly 10% of the CELS in other datasets. This improves differentiation between land use and land cover classes.

The *MapBiomas* 1.0 Collection provides annual land use and land cover (LULC) maps for Ecuador at a 30-meter resolution. These maps are generated through supervised classification using the Random Forest algorithm applied at the pixel level, based on satellite image mosaics from the Landsat series 4, 5, 7, 8, and 9. It uses a standardized legend tailored to Ecuador's specific land cover, dividing land into five main categories: Forest Formation, Non-Forest Natural Formation, Agriculture and Livestock Areas, Non-Vegetated Areas, and Water Bodies (Table 1). Natural forests fall under Forest Formation, while forest plantations, including silviculture, are classified as Agriculture and Livestock Areas. For detailed LULC category definitions, see Borja et al. (2023).

2.3 LULC change analysis and prediction by 2030

To achieve the objectives of this study, LULC maps from 2018 to 2022 were obtained from the MapBiomas platform and relevant explanatory variables related to LULC changes were generated using official data sources. The LULC maps from 2018 to 2022 were used to perform the LULC change analysis. Additionally, the LULC maps from 2018, 2020, and 2022, along with explanatory variables maps, were used to develop and validate a model designed to predict LULC changes through simulations up to 2030. The LULC change analysis, modeling, validation, and simulations were performed using the MOLUSCE tool (Figure 2).

Table 1. Classification of categories by land uses and land covers.

N°	Categories	Land Use/ Land Cover
1	Forest formation	Forest, open forest, mangrove and floodable forest.
2	Non-forest natural formation	Non-Forest wetland, grassland, rocky outcrop, other non-forest formations
3	Agriculture and Livestock Areas	Silviculture, Mosaic of cropland and pasture
4	Non-Vegetated Areas	Mining, urban areas, other non-vegetated areas
5	Water Bodies	Rivers, lakes, glaciers, aquaculture

2.3.1 LULC changes analysis

To describe LULC changes from 2018 to 2022, MapBiomas LULC maps were analyzed at one-year intervals. This analysis enabled the identification of historical LULC changes, detecting trends, and calculating LULC's annual rate of change. MOLUSCE tool was used to compute the transition matrix from 2018 to 2022, and the annual rate of change was calculated using Equation 1 (Puyravaud, 2003), originally proposed for deforestation studies but applicable to any LULC change due to its general formulation (Kouassi et al., 2021). Where q is the annual rate of change (1/year or %/year), A_1 is the LULC area at year t_1 and A_2 is the LULC area at year t_2, with $t_2 > t_1$.

$$q = \left(\frac{A_2}{A_1}\right)^{\dfrac{1}{t_2 - t_1}} - 1 \qquad (1)$$

2.3.2 MOLUSCE

The MOLUSCE tool was used to analyze and simulate LULC changes up to 2030. This QGIS plugin allows for calculating transition matrices and incorporates widely accepted algorithms for modeling and simulations, such as Artificial Neural Networks (ANN), Cellular Automata (CA), and the Kappa coefficient for validating the accuracy; this index ranges from 0 to 1, which is interpreted as poor and almost perfect, respectively (Gaur and Singh, 2023; Jain, 2024; Mollocana Lara and Paredes Obando, 2024). These algorithms have been widely applied in LULC modeling studies, such as those conducted by Souza et al. (2020); Xu et al. (2024).

ANN learns spatial patterns and relationships between historical data and explanatory variables, modeling the transition potential and CA simulates dynamic spatial processes by applying transition rules based on neighborhood conditions (Alipbeki et al., 2024; Tenorio et al., 2022).

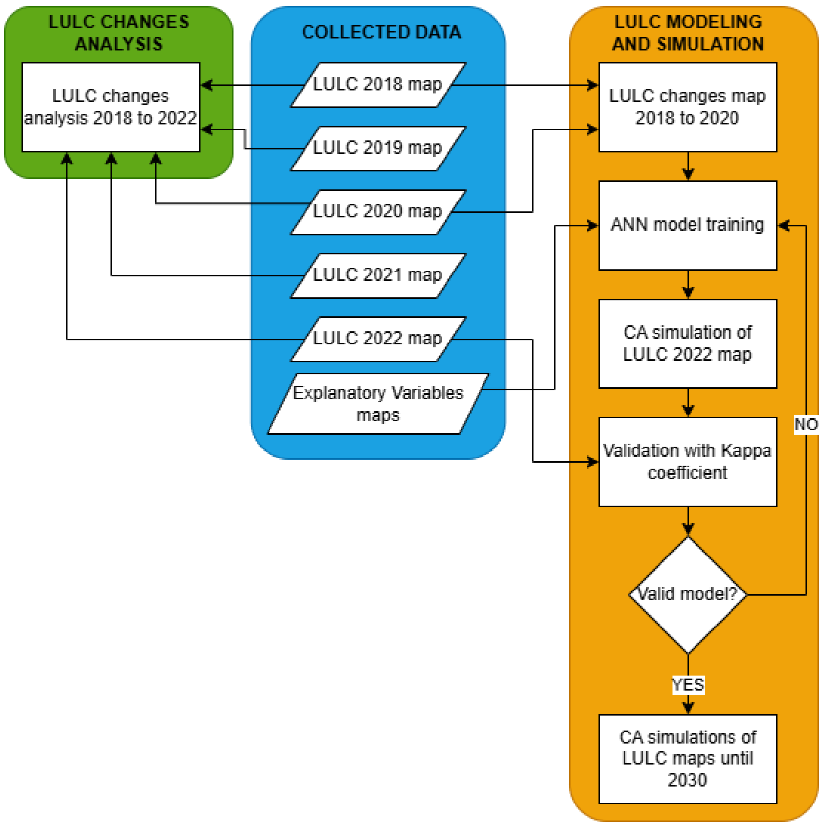

Figure 2. Methodology diagram for LULC analysis and prediction.

To predict LULC maps using the MOLUSCE tool, it is necessary to collect cartographic information representing explanatory variables related to LULC changes. This allows the Artificial Neural Network (ANN) algorithm within MOLUSCE to consider these variables during training, replicating learned behaviors and identifying spatial patterns (Al Mazroa et al., 2024). Five explanatory variables in raster format related to LULC changes were generated and integrated into the MOLUSCE tool. These variables are shown in Table 2.

Table 2. Definitions of explanatory variables for ANN training.

Variable	Definition
Proximity to roads	Raster representing the Euclidean distance in meters from each pixel to the nearest road
Proximity to settlements	Raster representing the Euclidean distance in meters from each pixel to urban centers
Protection level of natural areas	Raster representing the protection level of natural areas against natural cover removal on a scale from 0 to 5, where 0 indicates non-protected areas and 5 represents the highest level of protection
Altitude	Raster showing the height above sea level (m.a.s.l) for each pixel
Slope	Raster indicating the steepness or incline of the land for each pixel in degrees

Previous studies have identified proximity to roads and urban centers as key drivers of LULC change, as areas closer to these features tend to experience higher rates of natural cover loss due to increased accessibility and human activity (Gaur and Singh, 2023). Vegetation closer to roads and populated areas is more susceptible to removal due to the expansion of the agricultural frontier and the creation of pastures for livestock (Fischer et al., 2021).

Topographic features such as elevation and slope play an important role in determining the suitability of land for agriculture and development, as human activities are restricted or face difficulties in high-altitude or steep-slope areas (Xu et al., 2024). A significant portion of CELS is under some form of legal conservation, which acts as a major barrier against the advance of anthropogenic activities.

These explanatory variables are commonly used in LULC modeling because they can be obtained from accessible cartographic sources. In contrast, socioeconomic, law enforcement, or policy factors are less used due to data scarcity, complexity of spatial representation, and temporal mismatches. Despite these limitations, several studies have demonstrated good modeling results using only topographic and infrastructure variables, as seen in Barbosa de Souza et al. (2023); Alipbeki et al. (2024); Hasan et al. (2020).

While many studies have explored how protected areas help prevent deforestation, fewer studies have integrated protection levels as a variable in land use change models (Kim and Anand, 2021). Given that the CELS includes various types of protection and conservation areas, the protection level was integrated into the analysis to assess its influence on LULC dynamics. This level was determined through surveys conducted with three experts who were asked to evaluate, on a scale from 1 to 5, the effectiveness of different protection categories within the CELS in preventing deforestation. In this scale, 1 represents a low level of protection, while 5 indicates a high level of protection against deforestation.

For modelling and prediction purposes, a transition matrix from 2018 to 2020 (two-year interval) was calculated using the MOLUSCE tool. This matrix was used by MOLUSCE to create a change map, which, together with the explanatory variable rasters, served as inputs for the training of the ANN model that iteratively assesses its prediction accuracy and adjusts its structure to minimize errors. On the other hand, CA generates simulations based on the trained ANN model (Mustafa et al., 2021). In this study, each iteration of the CA algorithm produces a predicted LULC map two years in advance. The first iteration generated a LULC map for 2022, which was compared to the actual 2022 LULC map from MapBiomas to validate the model. Subsequently, four additional iterations were performed to produce a predicted LULC map for 2030. A transition matrix from the predicted LULC map for 2022 to that of 2030 was then calculated to analyze LULC changes and estimate annual rates of change using Equation 1.

After training the ANN model and generating a predicted LULC map for 2022 using the CA algorithm, it is essential to verify that the predictions made with the Cellular Automata algorithm and the ANN model are reliable enough to support decision-making (Bao Pham et al., 2024). To ensure this, the model was validated by comparing the predicted LULC map for 2022 generated by the algorithm with the actual LULC map from MapBiomas for the same year. The comparison was performed using Cohen's Kappa coefficient, a widely used metric for spatial data comparison (Mollocana Lara et al., 2021). MOLUSCE allows for multiple iterations of Kappa coefficient calculations, reducing errors caused by random sampling. The interpretation of the Kappa coefficient follows the criteria established in Santos et al. (2020).

3 Results and Discussion

3.1 LULC Changes Analysis from 2018 to 2022

The dynamics of land use and land cover change in the Llanganates-Sangay Connectivity Corridor (CELS) between 2018 and 2022 (Figure 3), shows the gradual decrease of Forest Formation areas stands out, especially in the CELS buffer zones. This suggests a process of deforestation, probably associated with human activities such as agricultural and livestock expansion, since this type of use shows a notable increase in the same area, indicating that the areas peripheral to the CELS have greater anthropic pressure. This change implies a significant transformation of forest ecosystems into more intensive uses.

The gradual loss of Forest Formation suggests an increase in landscape fragmentation, which affects ecological connectivity between montane and Amazonian ecosystems (Jokisch and Lair, 2002). Water Bodies and Non-Vegetated Areas remain relatively constant, with no perceptible changes in their extension, while Non-Forest Natural Formations show minor variations, which may be related to degradation or regeneration processes.

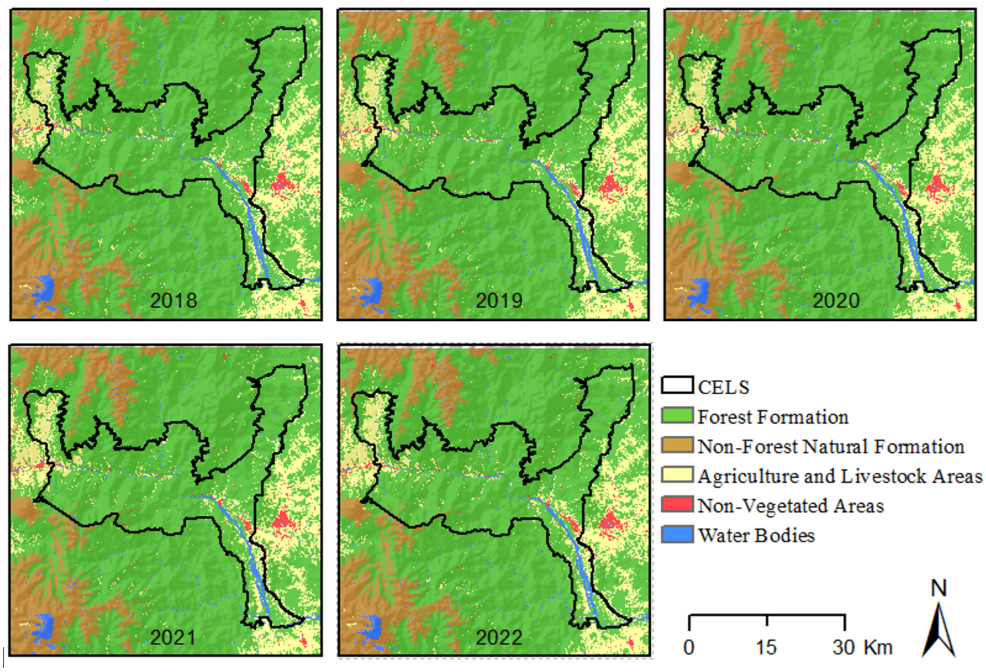

Figure 3. MapBiomas LULC maps from 2018 to 2022 (MapBiomas, 2024).

Table 3 and Figure 4 highlight the changes in LULC in CELS between 2018 and 2022, quantifying the transformation of the landscape. The Forest Formation category experienced an accumulated loss of 1,147.33 hectares, with an average annual rate of change of -0.37 %, and its maximum value in 2021-2022 with -515.03 hectares (-0.67 %/year).

This dynamic of decrease in the categories related to natural vegetation confirms that agriculture is the main driver of land use change, contributing significantly to deforestation and pressure on forest ecosystems that lose their ecological function in maintaining the diversity and connectivity of the landscape. Agricultural expansion, in turn, responds to economic stability that produces short-term fluctuations in the market.

Non-Vegetated Areas increased by 250.84 hectares (+8.50 %/year), showing their greatest growth between 2021-2022 (+107.31 ha, +13.52 %/year). This increase may reflect soil degradation processes related to erosion, urbanization and land abandonment, which alter the functionality of the corridor and generate a growing threat to natural ecosystems; this trend is consistent with other studies carried out in the Ecuadorian Amazon (Gutiérrez et al., 2016; Calvas et al., 2024; Viteri-Basso et al., 2024).

Table 3. CELS Land Use/Land Cover changes from 2018 to 2022.

Categories	Units	2018 to 2019	2019 to 2020	2020 to 2021	2021 to 2022	2018 to 2022
Forest Formation	ha	-266.94	-263.28	-102.09	-515.03	-1147.33
	q	-0.34	-0.34	-0.13	-0.67	-0.37
Non-Forest Natural Formation	ha	-8.96	-18.84	-7.32	5.12	-30.01
	q	-1.37	-2.92	-1.17	0.83	-1.17
Agriculture and Livestock Areas	ha	223.39	234.64	149.02	299.14	906.19
	q	2.26	2.32	1.44	2.85	2.21
Non-Vegetated Areas	ha	49.49	41.53	52.51	107.31	250.84
	q	7.61	5.94	7.09	13.52	8.50
Water bodies	ha	3.02	5.95	-92.12	103.46	20.31
	q	0.10	0.20	-3.09	3.58	0.17

*Negative symbol represents area reduction; ha represents change in hectares and q represents annual rate of change in %/year.

For their part, Water Bodies showed significant fluctuations, with losses in 2020-2021 (-3.09 %/year) and a partial recovery in 2021-2022 (+3.58 %/year). These dynamics, probably influenced by seasonal variations and sedimentation, require continuous hydrological monitoring to understand their causes and effects on the corridor.

Table 4 corresponds to the LULC transition matrix from 2018 to 2022. 96.93 % (75577.18 ha) of the area occupied by the Forest Formation category remained stable, 2.49 % changed to Agriculture and Livestock Areas and 0.15 % to Non-Vegetated Areas. This reflects the fact that agricultural expansion is the main driver of deforestation.

The Non-Forest Natural Formation category has a permanence of 88.57 % (578.7 ha), 7.55 % changed to Forest Formation and 3.19 % to Agriculture and Livestock Areas. Contrary to the above, 87.17 % (8629.23 ha) remained as Agriculture and Livestock areas. They expanded by 1058.96 ha (10,7 %) from Forest Formation and by 100.9 ha (1,02 %) from Non-Vegetated Areas. This confirms that agriculture is the main transformation factor of the landscape of the non-vegetated areas 610,72 ha (93,95 %) remained as non-vegetated areas, an increase of 120.57 ha (0,15 %) from Forest Formation and 64.49 ha (2,17 %) from Water Bodies, which could be associated with degradation and urbanization processes.

The category of water bodies has a permanence: 2589.5 ha (87,04 %) remained as water bodies, 64.49 ha (2,17 %) were reduced to non-vegetated areas and 130.54 ha (4,39 %) to forest formation, possibly due to changes in water dynamics, sedimentation, seasonal timing of the Landsat satellite images used in the MapBiomas classification or inherent algorithmic errors.

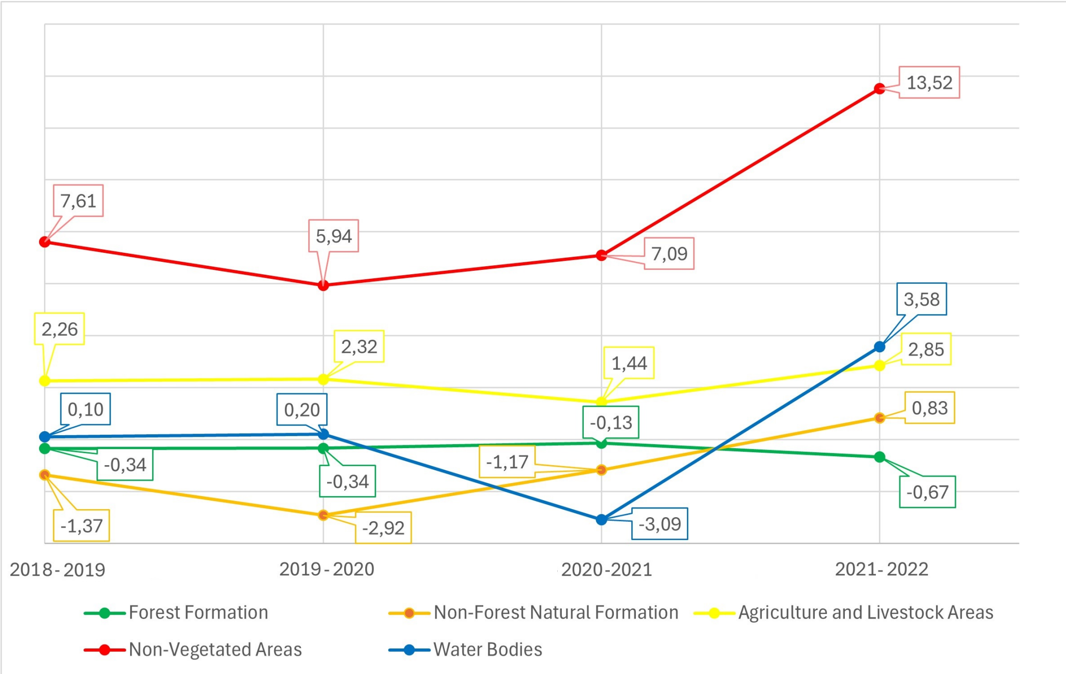

Figure 4. Evolution of annual LULC change rates (q %/year) at one-year intervals from 2018 to 2022.

The transition matrix shows that deforestation and conversion to agricultural land are the predominant dynamics in the CELS, driven by agricultural expansion. Additionally, the increase in non-vegetated areas reflects degradation processes that could intensify if sustainable management measures are not implemented.

Since Forest Formation annual rates of change are low, observing its area decrease (deforestation) is difficult. To improve this understanding, Figure 5 highlights the differences in Forest Formation changes between 2018 and 2019, as well as between 2018 and 2022.

3.2 Explanatory variables for 2030 LULC prediction

The rasters representing the explanatory variables for the prediction model are depicted in Figure 6 and Figure 7. Rasters proximity to roads, proximity to settlements, altitude and slope were generated from Military Geographic Institute (IGM) official information. The raster level of protection was generated based on information from the Ministry of Environment, Water, and Ecological Transition (MAATE), a conservation NGO supporting private areas in the CELS, and the expert opinions about the effective level of protection of different kinds of protected areas.

Not all conservation areas have the same level of protection against deforestation and the type of conservation areas varies significantly. Some are part of the National System of Protected Areas (SNAP), regulated by the Organic Environmental Code, which provides a robust legal framework that supports the conservation of these areas, and they have greater financial and technical capacity, which increases their level of protection. However, their effectiveness can be compromised by extractive activities permitted under legal exceptions, such as mining exploitation in certain protected areas.

Areas managed by local governments (GAD) have fewer resources and technical support, which limits their ability to implement effective conservation measures. In the case of privately owned areas, in some cases they are successful conservation models, which depend mainly on the commitment of the owners and lack a consolidated monitoring framework (Mendoza-Montesdeoca et al., 2022; Mestanza-Ramón et al., 2020).

Table 4. Transition matrix for LULC between 2018 and 2022.

2018 - 2022 Period	Forest formation	Non-forest natural formation	Agriculture and Livestock areas	Non-Vegetated areas	Water bodies	Total 2018
Forest formation	75577.18 (96.93 %)	23.6 (0.03 %)	1941.1 (2.49 %)	120.57 (0.15 %)	311.3 (0.4 %)	77973.75 (100 %)
Non-forest natural formation	49.31 (7.55 %)	578.7 (88.57 %)	20.86 (3.19 %)	4.21 (0.64 %)	0.27 (0.04 %)	653.34 (100 %)
Agriculture and Livestock areas	1058.96 (10.7 %)	19.03 (0.19 %)	8629.23 (87.17 %)	100.9 (1.02 %)	91.48 (0.92 %)	9899.6 (100 %)
Non-vegetated areas	10.43 (1.6 %)	0.37 (0.06 %)	25.71 (3.95 %)	610.72 (93.95 %)	2.84 (0.44 %)	650.05 (100 %)
Water bodies	130.54 (4.39 %)	1.65 (0.06 %)	188.9 (6.35 %)	64.49 (2.17 %)	2589.5 (87.04 %)	2975.09 (100 %)
Total 2022	76826.42	623.34	10805.80	900.89	2995.3	
Variation from 2018 to 2022	-1147.33	-30.01	906.19	250.84	20.31	

*The changes are expressed in hectares, with percentages in parentheses. Positive variation values indicate area gains, and negative values indicate losses.

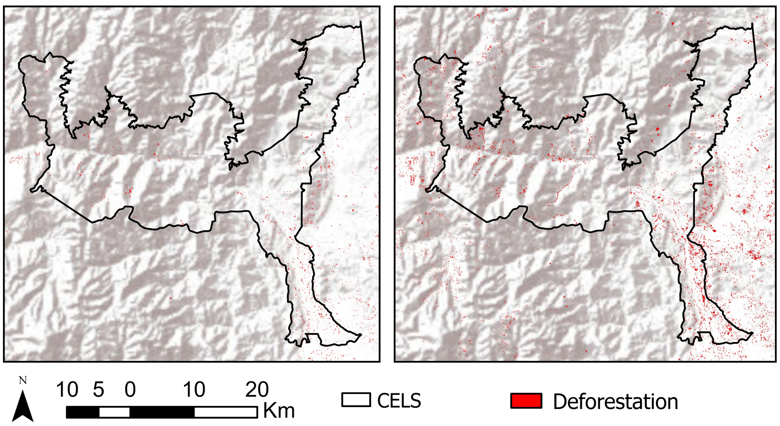

Figure 5. Deforestation represented as the transition from the Forest Formation class to any other LULC category between 2018–2019 (left) and 2018–2022 (right).

To account for these differences, three experts were polled to assess the level of protection against deforestation across various types of conservation areas. Selected experts have at least five years of experience in conservation and come from different institutions across Ecuador that have worked on officially recognized connectivity corridors (MAATE and two different NGO), providing varied perspectives and a broader understanding of conservation practices and challenges throughout the country. The results are presented in Table 5. Each protection level was rated on a scale of 1-5, with a value of 0 used for non-protected areas.

The importance of incorporating the protection level of a protected area into the model (Barreto et al., 2017; Pessôa et al., 2023) is demonstrated in Table 6, which shows its significant influence on deforestation rates. The annual change rates were calculated using the Equation 1. As expected, areas without any form of protection (protection level 0) experience the highest deforestation rates, followed by the Provincial Sustainable Development Ecological Area of Pastaza Province GAD (AEDSP), where sustainable productive activities are permitted (protection level 2). In contrast, protected areas such as ACMUS, APH, and Protective Forests (protection level 3) exhibit the lowest annual deforestation rates, followed by private protected areas (protection level 1).

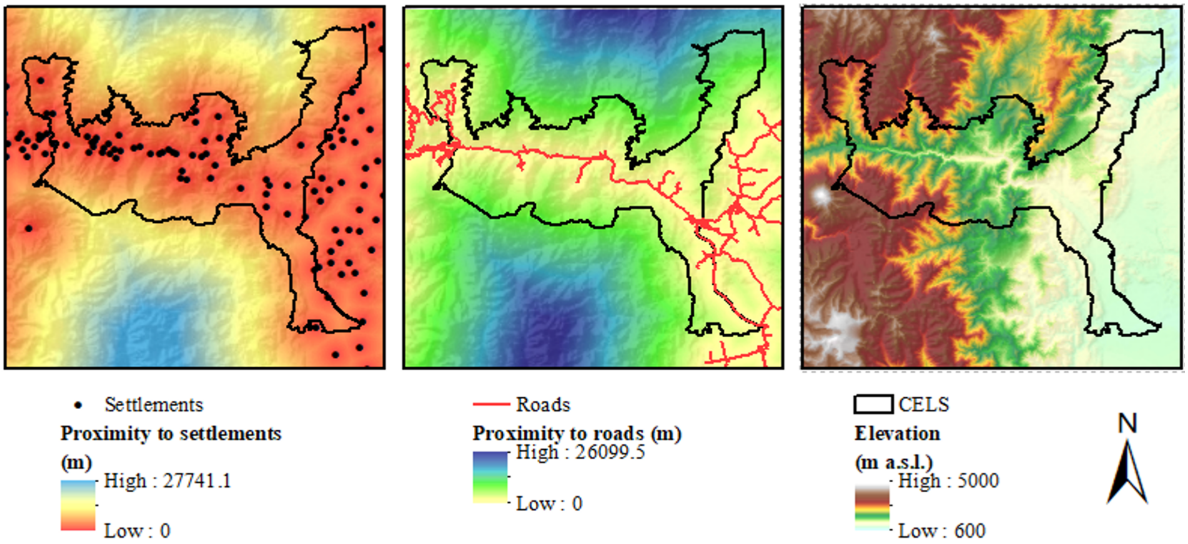

Figure 6. Proximity to settlements, proximity to roads and elevation explanatory variables.

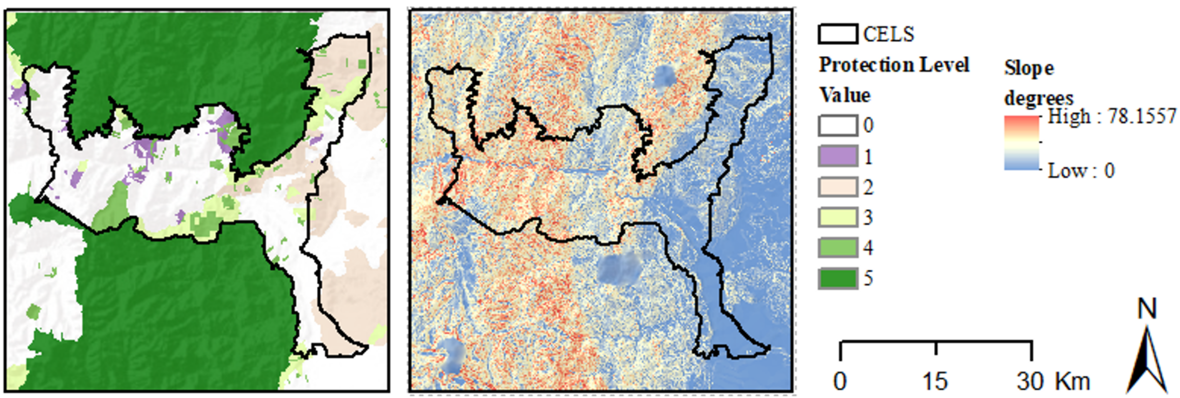

Figure 7. Protection level and slope explanatory variables.

Private protected areas exhibit a notable difference between the protection level reported by experts and the low deforestation rates calculated in this analysis. Two of the interviewed experts base their opinions on the lack of legal guarantees for long-term protection, as conservation status in private areas can change depending on the owner's vision. However, these areas often achieve higher conservation outcomes due to their specific focus, adaptability, and management by non-governmental organizations, families, or consortia, which implement rigorous conservation practices and reduce direct anthropogenic pressure. Despite these advantages, challenges persist, including tensions with local communities over restricted access to traditional resources and the vulnerability of conservation approaches to changes in ownership priorities (Iñiguez-Gallardo et al., 2021).

3.3 Artificial Neural Network model training

The ANN algorithm in the MOLUSCE tool was configured with a neighborhood size of 2 pixels and a learning rate of 0.002. Additionally, the momentum was set to 0.002 when these parameters help to stabilize learning and accelerate convergence. Figure 8 displays the learning curve illustrating the training process of the algorithm over 2000 iterations, with each iteration using 40,000 stratified sampling points to train and validate the neural network. The minimum error achieved by the neural network was 8.46 %.

Table 5. Results of a survey assessing the level of protection against deforestation, with 1 representing low level of protection and 5 high level of protection.

Type of conservation area	**Protection level**			
	Grade 1[a]	**Grade 2[b]**	**Grade 3[a]**	**Rounded average**
Private conservation areas	1	1	2	1
GAD conservation areas (ACMUS)	3	4	3	3
Water Protection Areas (APH)	3	3	4	3
Socio Bosque Program	4	4	3	4
Provincial Sustainable Development Ecological Area of Pastaza (AEDSP)	2	2	2	2
Protective Forests and Vegetation	1	4	4	3
National Parks (part of the SNAP)	5	5	5	5
Private Protected Areas (part of the SNAP)	3	5	5	4

[a]Specialists in Conservation- NGO.
[b]Specialist in Protected Areas– MAATE.

Table 6. Forest Formation annual rate of change according to the level of protection against deforestation of protected areas from 2018 to 2022.

Level of protection	**Forest formation 2018**	**Forest formation 2022**	**Change 2018- 2022**	
	ha	ha	ha	q (%/año)
0	42952.59	41962.24	-990.35	-0.58
1	3730.25	3727.59	-2.65	-0.02
2	13003.95	12889.33	-114.62	-0.22
3	9269.31	9264.46	-4.85	-0.01
4	8911.26	8876.59	-34.67	-0.10
5	106.39	106.21	-0.18	-0.04
Total	77973.75	76826.42	-1147.33	-0.37 %

*Negative values indicate area reduction.

3.4 Cellular Automata simulation

The predicted LULC maps from 2022 to 2030, at two-year intervals, are illustrated in Figure 9, while Table 7 details the transition for LULC predictions between 2022 and 2030 in hectares, with percentages in parentheses. Positive variation values indicate area gains, negative values indicate losses. Additionally, Figure 9 shows the evolution of predicted annual LULC change rates (%/year) at two-year intervals from 2022 to 2030 while Table 7 presents the corresponding transition matrix. In the other hand, Figure 10 shows the predicted future trends and variations in annual change rates of LULC categories from 2022 to 2030.

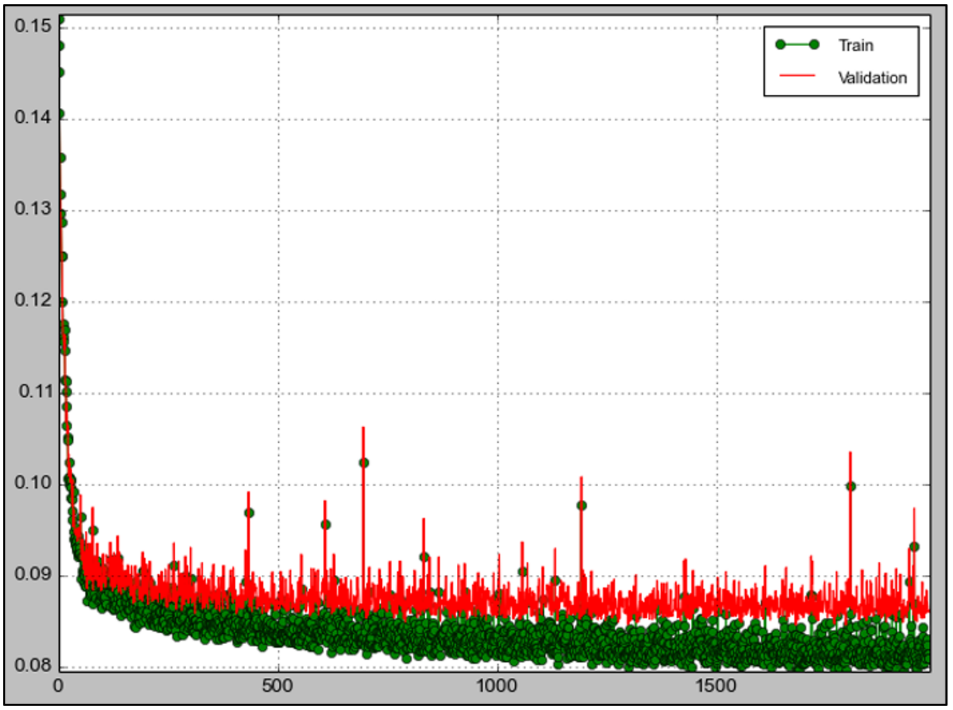

Figure 8. Artificial Neural Network learning curve.

Forest Formation, the largest land use, shows an area decrease (negative change rates), from 77025.39 ha in 2022 to 75396.42 ha in 2030, indicating ongoing but low reduction in forest cover, likely due to deforestation (Souza et al., 2020). The conversion of forests into pastures, agricultural land, and infrastructure is a key driver of deforestation, causing effects on ecosystems and climate. This process accelerates biodiversity loss, disrupts water systems, and releases stored carbon, intensifying climate change and altering local and regional environmental conditions (Kumar et al., 2022). Although most Forest Formation areas (95.59 %, 73628.13 ha) remained intact in the simulation, 3.72 % transitioned to Agriculture and Livestock Areas.

Similarly, 59.7 % of Non-Forest Natural Formations in 2022 persisted, while 21.04 % shifted to agriculture, indicating significant pressure on these ecosystems due to agricultural growth (Table 7). Decline in Non-Forest Natural Formation can lead to significant ecological consequences, including biodiversity loss and ecosystem degradation. For instance, the reduction of natural wetlands has been linked to decreased habitat quality and fragmentation, further exacerbating environmental degradation (Wilson et al., 2016).

Agriculture and Livestock Areas expand steadily, from 10804.52 ha in 2022 to 12582.78 ha in 2030, reflecting agricultural encroachment. Although Agriculture and Livestock Areas remained predominantly stable in the simulation (83.72 %, 9,045.19 ha), 1412.07 ha transitioned to Forest Formation. This shift may indicate the influence of conservation efforts and initiatives implemented in the CELS, such as promoting agroecological practices, which can facilitate forest restoration (Knapp and Sciarretta, 2023). Agriculture and Livestock Areas show positive but slightly deaccelerating change rates, indicating a continuous increase in agricultural land, albeit at a slower pace over time.

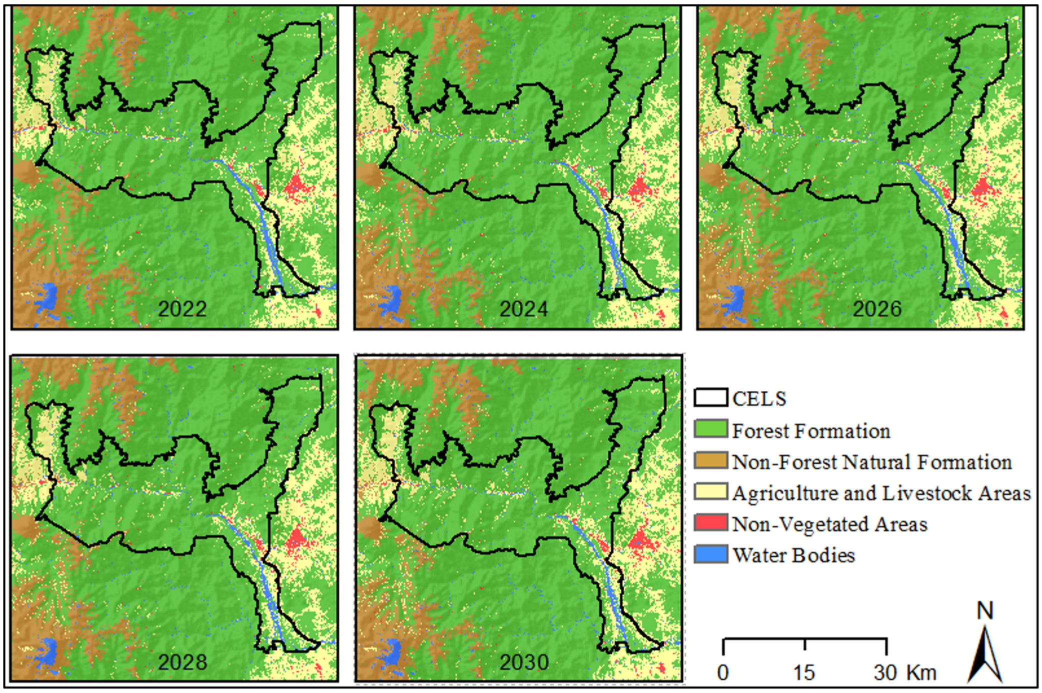

Figure 9. Predicted LULC maps from 2022 to 2030.

Table 7. Transition matrix for LULC predictions between 2022 and 2030.

2022 - 2030 Period	Forest formation	Non-forest natural formation	Agriculture and Livestock areas	Non-Vegetated areas	Water bodies	Total 2022
Forest formation	73628.13 (95.59 %)	82.88 (0.11 %)	2866.5 (3.72 %)	97.52 (0.13 %)	350.37 (0.45 %)	77025.39 (100 %)
Non-forest natural	112.06 (18.76 %)	356.68 (59.7 %)	125.69 (21.04 %)	2.01 (0.34 %)	1.01 (0.17 %)	597.45 (-100 %)
Agriculture and	1412.07 (13.07 %)	74.92 (0.69 %)	9045.19 (83.72 %)	130.45 (1.21 %)	141.88 (1.31 %)	10804.52 (100 %)
Non-vegetated areas	15.73 (2.1 %)	17.29 (2.31 %)	163.84 (21.86 %)	537.81 (71.77 %)	14.73 (1.97 %)	749.4 (-100 %)
Water bodies	228.42 (7.71 %)	2.2 (0.07 %)	381.56 (12.87 %)	41.99 (1.42 %)	2309.48 (77.93 %)	2963.65 (100 %)
Total 2030	75396.42	533.96	12582.78	809.77	2817.47	
Variation from 2022 to 2030	-1628.97	-63.49	1778.26	60.38	-146.18	

*The changes are expressed in hectares, with percentages in parentheses. Positive variation values indicate area gains, and negative values indicate losses.

In contrast, Non-Vegetated Areas exhibit positive and increasing change rates, reflecting a gradual expansion, likely associated with peri-urban growth (Souza et al., 2020) and other anthropogenic activity. This expansion could be also influenced by landslides and the increase in exposed river sandbanks, which become visible because of decreases in water bodies. Non-Vegetated Areas maintained 71.77% of their coverage, however, the conversion of 163.84 ha into Agriculture and Livestock Areas could be attributed to land reclamation and ecological restoration efforts facilitating their transition to productive agricultural landscapes (Zine et al., 2024).

Water Bodies, while maintaining 77.93% stability, experienced losses to both Forest Formation and Agriculture and Livestock Areas, likely driven by sedimentation processes and alterations in hydrological dynamics. Additionally, this trend may reflect the influence of the input data used to train the ANN, as the observed decline in Water Bodies from 2018 to 2022 appears to have guided the model to predict similar reductions in future scenarios. Further studies are needed to better understand the drivers behind these changes and to assess whether they represent temporary fluctuations, long-term trends, or potential errors in the modeling process. Figure 11 shows a comparison between the change from Forest Formation to any other LULC category between both periods 2022 - 2024 and 2022–2030.

3.5 Model validation

Using five iterations with 40,000 stratified sample points, an average Kappa coefficient of 0.95 was achieved, with stable values observed across all iterations. This indicates an excellent agreement between the predicted map and the 2022 MapBiomas map, suggesting that the model performs consistently and can be a useful tool in decision-making processes.

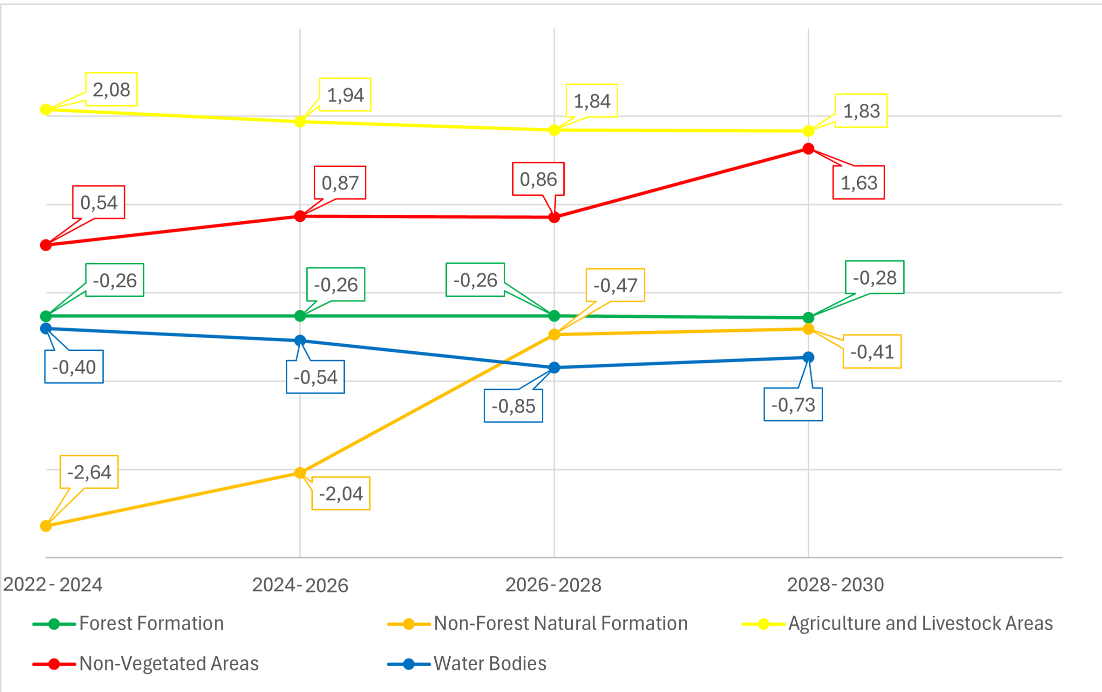

Figure 10. Evolution of predicted annual LULC change rates (%/year) at two-year intervals from 2022 to 2030.

3.6 Study limitations

The main limitations of this study include the low availability of satellite images due to the high cloud cover present during the analysis period. For this reason, land use and land cover maps generated by MapBiomas were used. Although this tool uses advanced image filtering and correction techniques, its cartography presents a margin of error with an accuracy of 80%. Likewise, the use of the MOLUSCE tool, despite its robustness and frequent application to generate trends, includes an associated margin of error, with a Kappa coefficient of 0.95.

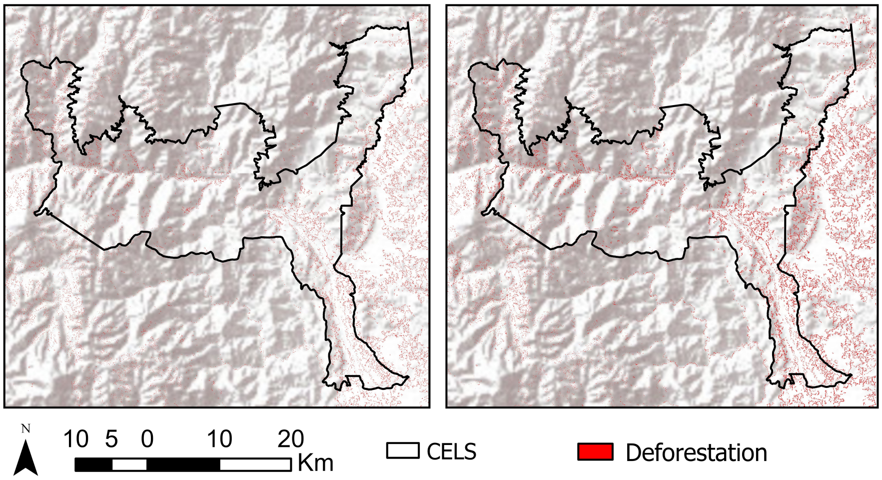

Figure 11. Predicted deforestation represented as the transition from the Forest Formation class to any other LULC category between 2022- 2024 (left) and 2022–2030 (right).

The naturalistic approach of the article prioritized the analysis of changes in natural cover and the different forms of conservation within the CELS. Socioeconomic, policy, political, and resource availability factors were not included in the analysis, due to the lack of readily available data and the complexities associated with integrating these variables into geospatial models. This represents an opportunity to carry out complementary research to address this limitation by incorporating data on population growth, economic activities, policy enforcement, resource availability and protected area management capacities to better capture the dynamics influencing LULC changes.

Despite these limitations, the results presented in this study reliably reflect the dynamics observed in the CELS. The variables used are widely applied in LULC modeling and the model was trained and validated using different data sets, reaching a high level of precision.

4 Conclusions

This study examined land use and land cover (LULC) maps sourced from the MapBiomas platform spanning 2018 to 2022. Predictive LULC maps for the period 2022 to 2030 were generated using the MOLUSCE tool in QGIS. Deforestation was represented as the transition from the Forest Formation class to any other LULC category. The findings confirm the expected trend of natural cover areas being replaced by anthropogenic uses, notably Agriculture and Livestock Areas expanding at the eastern and western boundaries of the CELS. To mitigate this, promoting sustainable anthropogenic practices such as agroecology is recommended.

Furthermore, it was observed that conservation areas exhibit lower deforestation rates, while most of the deforestation occurs in areas lacking any form of conservation status. Therefore, strengthening existing conservation areas, establishing new ones, and addressing the significant portion of unprotected natural cover within CELS are advisable strategies.

The relatively low deforestation rates found posed challenges in detecting changes in LULC maps. This challenge was also reflected in the Artificial Neural Network (ANN) algorithm, where training intervals had to be extended to two years due to minimal changes observed annually.

Using the ANN model and Cellular Automata simulation algorithm, the study estimated annual change rates between 2018 and 2022 as follows: a decrease of 0.37% per year, equivalent to 1147.33 hectares, for Forest Formation; a reduction of 1.17% per year, or 30.01 hectares, for Non-Forest Natural Formation; an increase of 2.21% per year, corresponding to 906.19 hectares, for Agriculture and Livestock Areas; a rise of 8.50% per year, representing 250.84 hectares, for Non-Vegetated Areas; and a slight increase of 0.17% per year, or 30.31 hectares, for Water Bodies. In contrast, LULC simulations for 2022 to 2030 predict an annual decrease of 0.27%, equal to 1628.97 hectares, for Forest Formation; a reduction of 1.39% per year, or 63.49 hectares, for Non-Forest Natural Formation; an increase of 1.92% per year, amounting to 1778.26 hectares, for Agriculture and Livestock Areas; a rise of 0.97% per year, adding 30.38 hectares, for Non-Vegetated Areas; and a slight decline of 0.63% per year, totaling 146.18 hectares, for Water Bodies. The model's predictive accuracy, evaluated using the Kappa coefficient, indicated excellent performance.

Acknowledgements

We extend our gratitude to the Hempel Foundation for funding the deforestation study in the Llanganates Sangay Connectivity Corridor, the process and results of which are presented in this article. We also thank WWF-Ecuador for their information and technical contributions. Special thanks go to the Universidad Politécnica Salesiana for its interest and efforts in disseminating knowledge about connectivity corridors, and to the CELS Research Network, of which ESPOCH is a part, for enabling this collaborative work opportunity.

Authors' contribution

L.J.J.C.: Conceptualization, Data curation, Formal analysis, Investigation, Methodology, Project administration, Supervision, Resources, Software, Validation, Visualization, Writing– original draft. A.C.M.H.: Conceptualization, Funding acquisition, Investigation, Methodology, Project administration, Resources, Supervision, Writing– original draft, Writing– review editing. A.C.G.G.: Formal analysis, Investigation, Methodology, Validation, Writing of introduction, methodology and results. J.G.M.L.: Data curation, Formal analysis, Investigation, Methodology, Validation, Visualization, Writing– review editing.

References

Admas, M. (2024). Predicting the impacts of land use/cover and climate changes on water and sediment flows in the megech watershed, upper blue nile basin. *Remote Sens*, 16:2385. Online:https://n9.cl/p2v51k.

Al Mazroa, A., Maashi, M., Kouki, F., Othman, K., Salih, N., Elfaki, M., and Begum, S. (2024). An analysis of urban sprawl growth and prediction using remote sensing and machine learning techniques for vila velha, brazil. *Journal of South American Earth Sciences*, 142:104988. Online:https://n9.cl/sseqj.

Alipbeki, O., Alipbekova, C., Mussaif, G., Grossul, P., Zhenshan, D., Muzyka, O., Turekeldiyeva, R., Yelubayev, D., Rakhimov, D., Kupidura, P., and Aliken, E. (2024). Analysis and prediction of land use/land cover changes in korgalzhyn district, kazakhstan. *Agronomy*, 14(2):268. Online:https://n9.cl/5tvd8.

Alvarado, O. (2020). La conservación neoliberal: otra cara de la economía verde. estudio de caso en el corredor ecológico llanganates sangay, ecuador. *Sociedad y ambiente*, (22):97–123. Online:https://n9.cl/0yycl.

Aneloa, W. E., Lara, J., Mendoza, C., Herrera, A., and Jacho, A. (2024). Development of a geoportal for the integrated management of cartographic information in the llanganates-sangay connectivity corridor. *Revista de Gestão Social e Ambiental*, 18(11):e08768. Online:https://n9.cl/wppfn.

Bao Pham, Q., Ajim Ali, S., Parvin, F., Van On, V., Mohd Sidek, L., Đurin, B., Cetl, V., Šamanović, S., and Nguyet Minh, N. (2024). Multi-spectral remote sensing and gis-based analysis for decadal land use land cover changes and future prediction using random forest tree and artificial neural network. *Advances in space research*, 74(1):17–47. Online:https://n9.cl/v4gdo.

Barbosa de Souza, K., Rosa dos Santos, A., Macedo Pezzopane, J., Machado Dias, H., Ferrari, J., Machado de Oliveira Peluzio, T., Toledo, J., Freire Carvalho, R., Rizzo Moreira, T., and França Araújo, E. (2023). Modeling dynamics in land use and land cover and its future projection for the amazon biome. *Forests*, 14(7):1281. Online:https://n9.cl/2egr1.

Barreto, J., González, T., and Armenteras, D. (2017). Dinámica espacio temporal de ocurrencia de incendios en zonas con diferentes tipos de manejo en el noroeste de la amazonia:¿ barrera efectiva? *Revista facultad de ciencias básicas*, 13(1):19–25. Online:https://n9.cl/susqb.

Borja, M., Holguín, W., Aguilar, C., Terán, K., Rodríguez, A., and Josse, C. (2023). Documento de bases teóricas de algoritmo (atbd) raisg - mapbiomas ecuador colección 1.0 de mapas anuales de cobertura y uso del suelo de ecuador. Online:https://n9.cl/89xt1.

Calvas, B., Castro, L., Kindu, M., Bingham, L., Pintado, K., Torres, J., Knoke, T., and Cueva-Ortiz, J. (2024). Large differences between observed and expected ecuadorian deforestation from 2001 to 2009: a counterfactual simulation approach. *Regional Environmental Change*, 24(2):1–15. Online:https://n9.cl/o4k9v.

Delgado Fernández, E., León Peralta, M., Cantos Guamán, C., and J., G. (2023). Effect of mining activity on biodiversity in a sector of the paquisha parish, province of zamora chinchipe-ecuador. *La Granja*, 38(2):106–123. Online:https://n9.cl/65gby.

Elagouz, M., Abou-Shleel, S., Belal, A., and El-Mohandes, M. (2020). Detection of land use/cover change in egyptian nile delta using remote sensing. *The Egyptian Journal of Remote Sensing and Space Science*, 23(1):57–62. Online:https://n9.cl/die101.

Fischer, R., Cordero, F., Luna, T., Velasco, R., DeDecker, M., Torres, B., Giessen, L., and Günter, S. (2021). Interplay of governance elements and their effects on deforestation in tropical landscapes: Quantitative insights from ecuador. *World Development*, 148:105665. Online:https://n9.cl/5x86g.

Gaglio, M., Aschonitis, V., Mancuso, M., Reyes Puig, J., Moscoso, F., Castaldelli, G., and Fano, E. (2017). Changes in land use and ecosystem services in tropical forest areas: a case study in andes mountains of ecuador. *Int. J. Biodivers. Sci. Ecosyst. Serv. Manag*, 13(1):264–279. Online:https://n9.cl/4q5fe.

Gaur, S. and Singh, R. (2023). A comprehensive review on land use/land cover (lulc) change modeling for urban development: current status and future prospects. *Sustainability*, 15(2):903. Online:https://n9.cl/9stqv.

Gutiérrez, R., Puig, J., Tapia, A., Terán, A., de Vargas, K., Bermudez, D., and Rodríguez, X. (2016). Desarrollo local y conservación en la vertiente oriental andina: corredor ecológico llanganates-sangay-valle del anzu. *Revista Amazónica. Ciencia y Tecnología*, 5(1):52–68. Online:https://n9.cl/wvv9v.

Hasan, S., Shi, W., Zhu, X., Abbas, S., and Khan, H. (2020). Future simulation of land use changes in rapidly urbanizing south china based on land change modeler and remote sensing data. *Sustainability*, 12(11):4350. Online:https://n9.cl/jhna4.

Heredia-R, M., Torres, B., Cabrera-Torres, F., Torres, E., Díaz-Ambrona, C., and Pappalardo, S. (2021). Land use and land cover changes in the diversity and life zone for uncontacted indigenous people: Deforestation hotspots in the yasuní biosphere reserve, ecuadorian amazon. *Forests*, 12(11):1539. Online:https://n9.cl/r3qb1.

Herrera, G. and Rodríguez, G. (2016). Resiliencia y turismo: El caso de la ciudad de baños de agua santa-ecuador. *Holos*, 3:229–250. Online:https://n9.cl/hso6tb.

INABIO, Ecominga Foundation, Sumak Kawsay In Situ, and Waska Amazonía (2023). *Amphibians and Reptiles of the Llanganates-Sangay Ecological Corridor*. National Biodiversity Institute Publication Series.

Iñiguez-Gallardo, V., Reyes-Bueno, F., and Peñaranda, O. (2021). Conservation debates: people's perceptions and values towards a privately protected area in southern ecuador. *Land*, 10(3):233. Online:https://n9.cl/147n4.

Jain, M. (2024). Future land use and land cover simulations with cellular automata-based artificial neural network: A case study over delhi megacity (india). *Heliyon*, 10(14):e34662. Online:https://n9.cl/zdry6.

Jokisch, B. and Lair, B. (2002). One last stand? forests and change on ecuador's eastern cordillera. *Geographical Review*, 92(2):235–256. Online:https://n9.cl/1o8235.

Jost, L. (2004). Explosive local radiation of the genus teagueia (orchidaceae) in the upper pastaza watershed of ecuador. *Lyonia*, 7(1):41–47. Online:https://n9.cl/kmuuf.

Kim, D. and Anand, A. (2021). Effectiveness of protected areas in the pan-tropics and international aid for conservation. *Geomatics*, 1(3):335–346. Online:https://n9.cl/m0dwx.

Kleemann, J., Zamora, C., Villacis-Chiluisa, A., Cuenca, P., Koo, H., Noh, J., Fürst, C., and Thiel, M. (2022). Deforestation in continental ecuador with a focus on protected areas. *Land*, 11(2):268. Online:https://n9.cl/8p6fh.

Knapp, J. and Sciarretta, A. (2023). Agroecology: protecting, restoring, and promoting biodiversity. *BMC Ecology and Evolution*, 23(1):29. Online:https://bit.ly/3Xgk2Ki.

Kouassi, J., Gyau, A., Diby, L., Bene, Y., and Kouamé, C. (2021). Assessing land use and land cover change and farmers' perceptions of deforestation and land degradation in south-west côte d'ivoire, west africa. *Land*, 10(4):429. Online:https://n9.cl/ke4z50.

Kumar, R., Kumar, A., and Saikia, P. (2022). *Environmental Degradation: Challenges and Strategies for Mitigation*, volume 104, chapter Deforestation and forests degradation impacts on the environment, pages 19–46. Springer.

Lukas, P., Melesse, A., and Kenea, T. (2023). Prediction of future land use/land cover changes using a coupled ca-ann model in the upper omo-gibe river basin, ethiopia. *Remote Sensing*, 15(4):1148. Online:https://n9.cl/o3xdi1.

Mainville, N., Webb, J., Lucotte, M., Davidson, R., Betancourt, O., Cueva, E., and Mergler, D. (2006). Decrease of soil fertility and release of mercury following deforestation in the andean amazon, napo river valley, ecuador. *Science of the Total Environment*, 368(1):88–98. Online:https://n9.cl/i2nwt.

MapBiomas (2024). Colección 1.0 de la serie de mapas anuales de cobertura y uso de suelo de ecuador. WebPage. Online: https://bit.ly/40GqWJu.

Mendoza-Montesdeoca, I., Rivera-Mateos, M., and Doumet-Chilán, Y. (2022). Políticas públicas ambientales y desarrollo turístico sostenible en las áreas protegidas de ecuador. *Revista de Estudios Andaluces*, (43):106–124. Online:https://n9.cl/eaxg3.

Mestanza-Ramón, C., Henkanaththegedara, S., Vásconez, P., Vargas, Y., Sánchez, M., Constante, D., Jimenez, M., Charco-Guamán, M., and Mestanza, P. (2020). In-situ and ex-situ biodiversity conservation in ecuador: A review of policies, actions and challenges. *Diversity*, 12(8):315. Online:https://n9.cl/56go9.

Mollocana Lara, J., Álvarez Mendoza, C., and Jaramillo Coronel, L. (2021). Evaluación de información relacionada con combustibles en el distrito metropolitano de quito para el modelado y simulación de incendios forestales, caso de estudio: Incendio del cerro atacazo. *La Granja. Revista de Ciencias de La Vida*, 34(2):45–62. Online:https://n9.cl/d57zh.

Mollocana Lara, J. and Paredes Obando, J. (2024). Assessment and selection of fuel models in areas with high susceptibility to wildfires in the metropolitan district of quito. In *International Conference on Innovation and Research*, pages 54–68. Online:https://n9.cl/j39e4z.

Muhammad, R., Zhang, W., Abbas, Z., Guo, F., and Gwiazdzinski, L. (2022). Spatiotemporal change analysis and prediction of future land use and land cover changes using qgis molusce plugin and remote sensing big data: a case study of linyi, china. *Land*, 11(3):419. Online:https://n9.cl/b0y84k.

Mustafa, A., Ebaid, A., Omrani, H., and McPhearson, T. (2021). A multi-objective markov chain monte carlo cellular automata model: Simulating multi-density urban expansion in nyc. *Computers, Environment and Urban Systems*, 87:101602. Online:https://n9.cl/1jt25.

Perea-Ardila, M., Leal-Villamil, J., and Oviedo-Barrero, F. (2021). Spectral characterization and monitoring of mangrove forests with remote sensing in the colombian pacific coast: Bajo baudó, chocó. *La Granja: Revista de Ciencias de la Vida.*, 34(2):27–44. Online:https://bit.ly/3CKfBA3.

Pessôa, A., Morelo, R., Silva-Junior, C., Doblas, J., Carvalho, N., Aragão, L., and Anderson, L. (2023). Protected areas are effective on curbing fires in the amazon. *Ecological Economics*, 214:107983. Online:https://n9.cl/82kct.

Puyravaud, J. (2003). Standardizing the calculation of the annual rate of deforestation. *Forest* *ecology and management*, 177(1-3):593–596. Online:https://n9.cl/yhlg7.

Reyes-Puig, J., Reyes-Puig, C., Pacheco-Esquivel, J., Recalde, S., Recalde, F., Recalde, D., Salazar, J., Peña, E., Paredes, S., Robalino, M., Flores, F., Paredes, V., Sailema, E., and Ríos-Alvear, G. (2023). First insights in terrestrial mammals monitoring in the candelaria and machay reserves in the ecuadorian tropical andes. *Biodiversity Data Journal*, 11:e98119. Online:https://n9.cl/bl2ojr.

Ríos-Alvear, G., Meneses, P., Ortega-Andrade, H., Santos, C., Muzo, A., López, K., Bentley, A., and Villamarín, F. (2024). Key connectivity areas in the llanganates-sangay ecological corridor in ecuador: A participative multicriteria analysis based on a landscape species. *Landscape and Urban Planning*, 246:105039. Online:https://n9.cl/w0pn4.

Rivas, C., Guerrero-Casado, J., and Navarro-Cerrillo, R. (2024). Functional connectivity across dominant forest ecosystems in ecuador: A major challenge for a country with a high deforestation rate. *Journal for Nature Conservation*, 78:126549. Online:https://n9.cl/msrhe.

Santos, F., Telles, L., Rosas, J., Gomes, A., Martins, R., Nascimento, A., and Sousa, E. (2020). Open source iterative bayesian classifier algorithm for quality assessment of processed coffee beans. *Nativa*, 8(1):118–123. Online:https://n9.cl/ugjvpj.

Souza, C., Z. Shimbo, J., Rosa, M., Parente, L., Alencar, A., Rudorff, B., Hasenack, H., Matsumoto, M., Ferreira, L., and Souza-Filho, P. (2020). Reconstructing three decades of land use and land cover changes in brazilian biomes with landsat archive and earth engine. *Remote Sensing*, 12(17):2735. Online:https://n9.cl/ybrqd.

Talukdar, S., Singha, P., Mahato, S., Pal, S., Liou, Y., and Rahman, A. (2020). Land-use land-cover classification by machine learning classifiers for satellite observations-a review. *Remote sensing*, 12(7):1135. Online:https://n9.cl/v7m3k.

Tenorio, C., Álvarez, G., Perez-Alania, M., Blanco, J., Paulino, C., Blanco, J., and Uribe, E. (2022). Bloom of prorocentrum cordatum in paracas bay, peru. *Diversity*, 14(10):844. Online:https://n9.cl/tkn7s.

Tikuye, B., Rusnak, M., Manjunatha, B., and Jose, J. (2023). Land use and land cover change detection using the random forest approach: The case of the upper blue nile river basin, ethiopia. *Global Challenges*, 7(10):2300155. Online:https://n9.cl/495uf.

Vergara, A., Arias, M., Gachet, B., Naranjo, L., Román, L., Surkin, J., and Tamayo, V. (2022). Informe de amazonía viva 2022. Technical report, WWF. Online:https://n9.cl/wov9ve.

Viteri-Basso, E., Puig, J., Reyes-Puig, C., and Ríos-Alvear, G. (2024). Shadows in the forest: Uncovering unusual colouration records in mammals from the ecuadorian tropical andes. *Biodiversity Data Journal*, 12:e137463. Online:https://n9.cl/z1aa5n.

Wilson, M., Chen, X., Corlett, R., Didham, R., Ding, P., Holt, R.and Holyoak, M., Hu, G., Hughes, A., and Jiang, L. (2016). Habitat fragmentation and biodiversity conservation: key findings and future challenges. *Landscape Ecology*, 31:219–227. Online:https://n9.cl/95fg8.

Xu, J., Jiao, C., Zheng, D., and Li, L. (2024). Agricultural land suitability assessment at the county scale in taiyuan, china. *Agriculture*, 14(1):16. Online:https://n9.cl/kiut6.

Zine, H., Hakkou, R., Papazoglou, E., Elmansour, A., Abrar, F., and Benzaazoua, M. (2024). Revegetation and ecosystem reclamation of post-mined land: toward sustainable mining. *Int. J. Environ. Sci. Technol.*, page 9775–9798. Online:https://n9.cl/rqhhbx.